Proceedings of the 20th International Conference on Soil Mechanics and Geotechnical Engineering– Rahman and Jaksa (Eds)

Simplified liquefaction triggering assessment of coral-derived carbonate sands

Évaluation simplifiée du déclenchement de la liquéfaction des sables carbonatés dérivé du corail

Merrick Taylor
Beca Ltd., Auckland, New Zealand, merrick.taylor@beca.com

Russell A. Green
Department of Civil & Environmental Engineering, Virginia Tech, Blacksburg VA, USA

ABSTRACT: The properties and behaviour of carbonate sands, which are found globally in tropical & sub-tropical environments, present geotechnical challenges where conventional design and assessment methods are based on the characteristics of predominantly terrestrial silica-derived soils, including the empirically derived simplified liquefaction assessment method. Owing to their mineralogy and typical granular characteristics, they exhibit high compressibility and are prone to crushing at relatively low pressures. For liquefaction assessment these properties affect the empirically derived simplified method. In this paper we explore methods to account for these effects on penetration test (SPT, CPT) and shear wave velocity (Vs) based triggering assessment methods. It was found that cyclic test results from a range of carbonate sands compare well to a state-based empirical triggering curve, indicating that the underlying physical basis for the simplified method remains useful for application to these soils. Application to case histories from the 1993 M 7.8 Guam and 2010 M 7.0 Haiti earthquakes provides further confidence in the approach.

RÉSUMÉ : Les propriétés et comportements des sables carbonatés, typiques des environnements tropicaux et sub-tropicaux, présentent des défis pour l'ingénierie géotechnique. Les méthodes conventionnelles de conception et d'évaluation sont basées sur les caractéristiques des sols principalement dérivés de la silice terrestre, notamment la méthode empirique simplifiée d'évaluation de liquéfaction. En raison de leur minéralogie et caractéristiques granulaires typiques, ils ont une compressibilité élevée et sont susceptibles d'être broyés à des pressions relativement faibles. Pour l'évaluation des risques, ces propriétés impactent la méthode empirique simplifiée d'évaluation de liquéfaction. Dans cet article, nous explorons les approches prennant en compte leurs effets sur les méthodes d'évaluation du déclenchement basées sur les tests de pénétration (SPT, CPT) et la vitesse des ondes de cisaillement (Vs). Les résultats des tests cycliques d'une gamme de sables carbonatés montrent une corrélation avec la courbe empirique de déclenchement basée sur l'état; indiquant que la base physique de la méthode simplifiée est valide pour son application aux sables carbonatés. L'application aux cas des tremblements de terre de Guam en 1993 et Haïti en 2010, respectivement de magnitude M 7.8 et M 7.0, renforce la confiance dans l'approche.

KEYWORDS: carbonate sand, liquefaction

1 INTRODUCTION

1.1 *Origin and geotechnical properties*

Carbonate sands of predominantly calcareous mineralogy [$CaCO_3$] are prevalent in tropical and sub-tropical environments globally. The soils are typically of bioclastic origin, formed from the skeletal remains of broken shells of marine organisms or through chemical precipitation (oolites). The geotechnical behaviour of carbonate sands has been extensively explored and reported on by Datta et al. (1980), Golighty & Hyde (1988), Semple (1988), Poulos (1988), Coop (1990), Coop & Atkinson (1993), Fioravante et al. (1994, 1998, 2013), Porcino et al. (2008), Brandes (2011), Van Impe et al. (2015), Giretti et al. (2018a, 2018b) among many others. Standard methods of soil characterisation and analysis are generally based on soils of siliceous mineralogy [SiO_2], and the differences between predicted and measured behaviour when applied to carbonate soils can be significant, including the liquefaction triggering assessment using the 'simplified method'. This is mainly due to the characteristics of carbonate soils, such as highly angular, weak crushable particles, high in-situ void ratios, and high compressibility. On the other hand, while some parameters lie outside those of silica soils such as the high friction angle ($\phi'_{cv} \sim 38 - 40°$) and very high λ/κ ratio (i.e. highly compressible beyond the yield stress, yet stiff upon unloading), the behaviour conforms to critical state soil mechanics (Coop, 1990).

Carbonate sediments may become lithified by cementation as a result of carbonate precipitation and growth of crystals on the surfaces of sediment grains, which can occur soon after deposition. The strength of cementation depends on water temperature, chemistry and depth. The cementation is irregular and generally develops in thin bands, so that significant vertical variation in the degree of cementation is not uncommon (Poulos 1988; Morioka & Nicholson 2000; Fioravante et al. 2013).

For lagoonal coral derived sediments deposited in back-reef environments, the development of weak cementation at grain contact points tends to result in a pseudo-stable soil mass, maintaining its loosely deposited structure despite external loads such as wave action and consolidation due to further deposition above (Nicholson, 2006). It may be (in part) responsible for increased small strain stiffness as measured in the field by shear wave velocity (V_S) not consistent with the in-situ void ratio. Weak cementation can lead to low strength characteristics, high compressibility, and cyclic sensitivity once the weak bonds are broken.

Left uncorrected these effects would be expected to translate to an overly conservative assessment of liquefaction resistance when applying either the Cone Penetration Test (CPT-) or Standard Penetration Test (SPT-) based simplified method, meaning more extensive liquefaction triggering would be predicted than would be expected to be observed, and conversely potentially unconservative assessment when applying the small-strain shear wave velocity (V_S-) based simplified method.

1.2 *Liquefaction resistance of carbonate sands*

Post-earthquake reconnaissance reports have documented the extensive damage to major ports on the Pacific Island of Guam following the 1993 M_w 7.8 earthquake (Mejia & Yeung, 1995), and in Port-au-Prince, Haiti following the 2010 M_w 7.0 earthquake (Rathje et al. 2010; Green et al. 2011), where reclamation fills comprising coralline soils liquefied and exhibited lateral spreading. Liquefaction of coralline soils has also been observed in Hawaii following the 2006 M_w 6.7 earthquake (Medley, 2006). An important note is that severe liquefaction was observed in loose fills placed as part of port reclamations, rather than in natural deposits.

In recent decades there has been significant interest from industry in the cyclic response of carbonate sands, owing to major offshore energy and/or reclamation projects in Australia, the Arabian Peninsula/ Persian Gulf and the South China Sea.

Research comparing the cyclic resistance of carbonate and silicate sands of the same relative density typically show either similar or higher cyclic resistance from carbonate sands, thought to be on account of the mineralogy, and highly angular grains (Hyodo et al. 1998; Morioka & Nicholson 2000; La Vielle 2008; Porcino & Marciano 2010; Brandes 2011; Pando et al. 2012). Due to these differences in behaviour, and perhaps more significantly due to the problem of grain crushing of carbonate materials during penetration testing, resulting in lower SPT *N* or CPT q_c values recorded than for a silica derived sand of the same relative density, D_R, (Morioka & Nicholson, 2000; Al Homoud &Wehr, 2006; Porcino & Marciano, 2010; Mayne, 2014; Van Impe, et al., 2015; Giretti et al. 2018b), the simplified method is either not adopted in favour of high quality sampling, cyclic laboratory testing, and numerical analysis (e.g. offshore energy industry), or its application heavily caveated without express consideration for these effects (Mejia & Yeung 1995; Nicholson 2006; Giretti et al. 2018a). In addition, an observed discrepancy between V_S-based liquefaction assessment and penetration-test based assessment procedures has been noted for carbonate deposits (Rollins et al. 2004; Nicholson, 2006). Measurements of both V_S and cyclic resistance in the laboratory show typically higher V_S values are measured for carbonate sands than expected from silica sands having the same cyclic resistance (Brandes, 2011; Porcino & Tomasello, 2019). This further implies V_S-based simplified liquefaction assessment methods may also not be appropriate in these materials without suitable corrections.

The remainder of this paper presents a proposed method that seeks to address the major concerns regarding these soils by adapting the simplified method for evaluating liquefaction triggering potential of carbonate sands in general, with application to carbonate sands having coralline origins in the Pacific and similar environments globally.

2 CORRECTIONS TO PENETRATION RESISTANCE

2.1 *Relative density-based corrections*

The use of D_R as a basis for corrections is fraught with reliability and applicability issues, one of which is the sensitivity of D_R to the void ratio limits, e_{min} and e_{max}. These limits are dependent on the methods used to determine maximum and minimum dry densities, respectively, which vary globally, and in the case of maximum density, may induce crushing in the process (Van Impe et al. 2015). Nevertheless, a simple approach that is sometimes used to account for the high compressibility and grain crushing of carbonate sands is to apply a so called 'shell correction factor': $SCF = q_{t1,silica}/\ q_{t1,calc} > 1$, where $q_{t1}= (q_t/\sigma_{atm})/(\sigma'_{v0}/\sigma_{atm})^{0.5}$ is the stress-normalised cone resistance similar to q_{c1N} (Idriss & Boulanger 2008). The *SCF* is used to derive a 'silica equivalent' normalised cone resistance value: i.e. $q_{t1,se} = SCF{\cdot}q_{t1,calc}$. The silica equivalent cone resistance may then be used with conventional correlations for siliceous sands, including simplified methods for estimating the liquefaction triggering potential of soils (Wehr 2005, Al-Homoud & Wehr 2006, Mayne 2014; Mengé et al. 2016). The *SCF* is typically derived from correlations relating q_c and D_R for both silica and calcareous sands, established from CPT calibration chamber (CC) testing. Early comparisons by Vesic (1965) and Bellotti & Jamiolkowski (1991) indicate *SCF* ratios of 1.3 to 2.2, with *SCF* increasing with D_R. Wehr (2005) presented a linear relationship as a function of D_R based on select CC data – carbonate Quiou sand (QS) and Palm Island (Dubai, UAE) sand compared to the siliceous Ticino sand (TS) from Italy, and Karlsruhe sand from Germany. It was stated as being applicable to low confining pressures ($p' < 100$ kPa, where p' is the mean effective confining stress) and for sands with median grain size, D_{50}, between 0.06 – 4 mm, noting that for higher p' and grain sizes the *SCF* tends to be higher. Mengé et al. subsequently investigated through CC testing other Persian Gulf sands and concurred with Wehr's findings - both the linear relationship proposed and the variation of *SCF* with p'. In both cases the *SCF* was used to establish criteria for field verification of the increase in density of hydraulic fill due to vibro-compaction.

However, CC testing of other carbonate sands appears to indicate significantly diverging results. Mayne (2014) collated CC data from six carbonate & calcareous sands: QS (France); Dogs Bay (Ireland); Kenya; Ewa Plains (Hawaii); Kingfish (Australia), and Jeju sands (Korea). These sands have varying biogenic origins (shell, coral, oolite) and were compared to CPT-based correlations for D_R established for silica sands; refer to Figure 1. From the ratio of the q_{t1}-D_R correlation for siliceous sands (e.g. Jamiolkowski et al. 2001), and the linear relationship, D_R [%] = $0.87q_{t1,calc}$, developed for carbonate sands, Mayne (2014) proposed the following *SCF*:

$$SCF = \frac{q_{t1,silica}}{q_{t1,calc}} = 6 - \frac{5}{1+\left(\frac{D_R[\%]}{100}\right)^4} \cong 6 - \frac{5}{1+\left(\frac{0.87q_{t1,calc}}{100}\right)^4} \quad (1)$$

A relationship between q_{t1} and D_R for carbonate sands was developed by adopting the equation form of Idriss & Boulanger (2008) and curve fitting to Mayne's CC dataset by minimising the sum of the square of the error, yielding a C_{dq} value of 0.5016, noting that Idriss & Boulanger (2008) adopted 0.9 for typical siliceous sands:

$$D_R = 0.465\left(\frac{q_{t1}}{C_{dq}}\right)^{0.264} - 1.063 \quad (2)$$

Note that other CPT-based D_R correlations for select carbonate sands have been presented by Jamiolkowski et al. (2001), Porcino & Marciano (2010), and Van Impe et al. (2015).

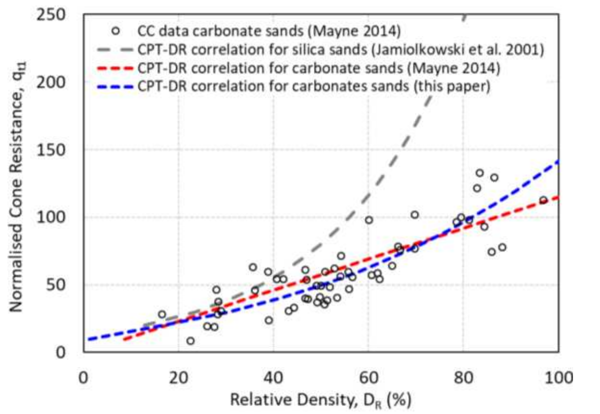

Figure 1. Calibration chamber (CC) test data for carbonate sands compared to CPT-D_R correlations for silica and carbonate sands.

The discrepancy between the *SCF*'s proposed by Wehr (2005) and Mayne (2014) for carbonate sands is significant (Figure 2). Most notably, for very dense sands ($D_R > 85\%$), the *SCF* ratio of Mayne reaches ~3.5 but only reaches 1.8 for Wehr. Conversely, for loose sands ($D_R < 30\%$), Wehr's *SCF* remains substantial at ~1.5, while Mayne's approaches unity. It is noted that the CC testing of Persian Gulf sands undertaken by both Wehr (2005) and Mengé et al. (2016) was limited to a D_R range of 40 - 70%, with the Wehr *SCF* relationship extrapolated linearly beyond these limits in Figure 2. Mayne's dataset extends from 16 – 98% and is better able to capture the non-linear characteristics of *SCF* at low and high densities.

The non-linear *SCF* appears to agree with our expectations from a state-based interpretation, where the density at critical state for carbonate sands is ~30% (at p' = 100 kPa), which may be estimated as follows (Boulanger 2003, after Bolton 1986):

$$D_{R,cs} = \frac{1}{\left(Q - \ln\left[\frac{100 \cdot p'}{Pa}\right]\right)} \quad (3)$$

where *Pa* is atmospheric pressure (~101 kPa), and *Q* is an empirical constant for the compressibility of the soil, depending on mineralogy and grain crushability characteristics intrinsic to the soil: *Q* ~7.5 carbonate sands (Randolph et al. 2004) and *Q* ~10 for quartz. This allows estimation of the critical state line (CSL) where laboratory test results establishing its position are not available.

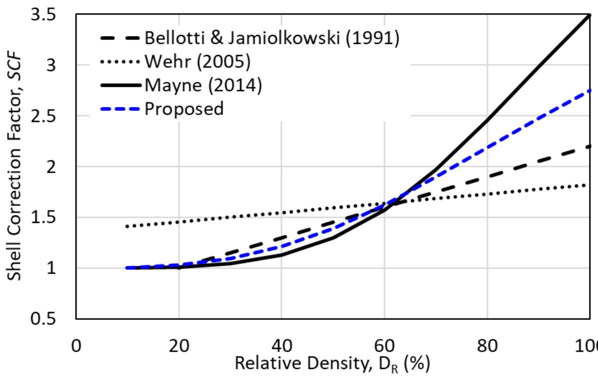

Figure 2. Comparison of Shell Correction Factors (SCF).

There is a degree of uncertainty in the D_R correlation (equation 2) due to the scatter in the CC data. This scatter is attributed to the variation in properties between different carbonate sands: gradation; particle shape; intra-particle voids, all related to their biogenic origins and affecting the strength to resist crushing. Other aspects may include variations in confining stresses applied, methodology of performing tests (including e_{max} and e_{min}), though as noted by Jamiolkowski et al. (2001) for highly compressible sands, the effect of chamber size and boundary conditions can be considered negligible. In lieu of site-specific characterisation (rare in practice), we suggest considering an average *SCF* curve from those of Bellotti & Jamiolkowski (1991) and Mayne (2014) (Figure 2), which is moderately-conservative and may be expressed as:

$$SCF = \frac{q_{t1,\text{silica}}}{q_{t1,\text{calc}}} = 4.5 - \frac{3.5}{1+\left(\frac{D_R[\%]}{100}\right)^3} \quad (4)$$

2.2 *Corrections for SPT testing*

While CPT is currently the preferred tool for characterising the geotechnical properties of alluvial soils for evaluating liquefaction resistance, SPT retains its use in engineering practice. Most notably the SPT is valuable where the CPT may meet refusal in some ground conditions (e.g., glacial deposits and gravely sands), where a CPT may be unavailable or otherwise uneconomical to mobilise (e.g. remote Pacific Islands), or where an important body of SPT data is available from previous ground investigations including case histories.

The *SCF* being based on a ratio of CPT q_c values implies that equation (4) may be applied to SPT values prior to application to the SPT-based simplified method, i.e. $(N_1)_{60,se} = SCF \cdot (N_1)_{60,calc}$. Direct application, however, is hampered by lack of a clear correlation between either N_{60} and D_R or q_c and N_{60} for carbonate sands. Lees et al. (2013) present q_c and uncorrected *N* data from Palm Jumeirah (Dubai, UAE) that indicates q_c/N = 0.4 for carbonate sand fill. However, the data have significant scatter and SPT hammer energy was not measured. Other studies in the Persian Gulf suggest either a similar range or widely varying values. We present the following alternative approach to develop an SPT-based D_R correlation for carbonate sands based on state concepts, where both the CC dataset collated by Mayne and the published CPT-based D_R correlations for carbonate (Mayne, 2014) and siliceous sands (Idriss & Boulanger, 2008) are transposed and plotted in terms of the relative state parameter, ξ_R, (Boulanger, 2003):

$$\xi_R = D_{R,cs} - D_R \quad (5)$$

ξ_R represents the distance in terms of D_R of the state of the soil from the CSL in D_R vs. p' space. Positive values of ξ_R represent contractive response for soils 'loose' of critical state, and negative values represent dilative response of soils 'dense' of critical state. D_{Rcs} was estimated for both siliceous and carbonate sands using equation (3). In the state-based framework both correlations compare well to the CC dataset, suggesting ξ_R may be adopted as a common reference for both types of sand. By equating ξ_R for both silica and carbonate sands, we can estimate the $D_{R,calc}$ by rearranging:

$$D_{R,\text{calc}} \cong \left(D_{R,cs,\text{calc}} - D_{R,cs,\text{silica}}\right) + D_{R,\text{silica}} \quad (6)$$

where: $D_{R,silica}$ = $[(N_1)_{60}/\ 46]^{0.5}$ with $(N_1)_{60}$ being the energy corrected, stress normalised SPT blow count (Idriss & Boulanger, 2008). It follows from equations (3) and (5) that at p' of 100 kPa, this reduces to:

$$D_{R,calc} \approx 0.159 + [(N_1)_{60}/46]^{0.5} \quad (7)$$

When equated to equation (2), this provides a median ratio of $q_{t1}/(N_1)_{60}$ of 8, with increasing values for lower densities and decreasing values for higher densities. A value of 8 is higher than implied by Lees et al. (2013) but does not seem unreasonable for sands.

Thus, for correcting SPT test data for the compressibility and grain crushing differences between silica and carbonate sands, we may adopt the suggested *SCF* in equation (4) as follows:

$$SCF = \frac{(N_1)_{60,silica}}{(N_1)_{60,\text{calc}}} \cong 4.5 - \frac{3.5}{1+\left(0.159+\sqrt{\frac{(N_1)_{60}}{46}}\right)^3} \quad (8)$$

2.3 *A state-based correction*

The advantage of adopting a state-based framework is to capture the influence of both density and confining stress conditions on soil behaviour, notably the stress-dilatancy response at large strains. A potential disadvantage of a state-based framework for liquefaction triggering assessment is that liquefaction as a phenomena is governed by moderate strain response over the majority of loading cycles during earthquake shaking, and only exhibits large strains as it approaches excess pore water pressure ratios > 80%. However, in the context of this paper it presents a step forward from adopting D_R-based shell correction factors. Therefore, instead of D_R, the state parameter ψ (Been & Jefferies, 1985) may be adopted either in the original form $\psi = e - e_{cs}$, (i.e. the distance in terms of void ratio that the state of soil is from critical state at the same mean effective stress), or some variant such as ξ_R per equation (5). Application requires deriving the state parameter from field test data (CPT, SPT) in carbonate sands (e.g., equations 3 & 5, used in conjunction with either equation 2 or 7), with the empirical liquefaction triggering curve transposed into state parameter space. Jefferies & Been (2006) have previously provided a correlation relating normalised cone resistance and ψ, and further expressed the liquefaction triggering curve in terms of cyclic resistance ratio, *CRR* and state parameter, ψ. Porcino & Marciano (2010) compared the liquefaction resistance of carbonate QS (which is comprised of a large % of broken shell), and siliceous TS, alongside the empirical triggering curve. They did this by transposing both the cyclic triaxial test results and triggering curve into *CRR*: ξ_R space. By utilising a direct correlation between CPT and D_R for QS (established from CC testing) and replotting the triggering curve in state-space, they avoided the need for an *SCF*. The results indicate similar trends for the triggering curve and TS, and a slightly higher cyclic resistance for QS. This difference is further explored herein by reviewing a wider array of carbonate sands, including coralline deposits.

3 EVALUATION OF CYCLIC STRENGTH TEST DATA

Published results of laboratory cyclic tests performed on carbonate sands have been collated in Table 1. The form of the results is cyclic strength 'fatigue' curves plotted as applied cyclic stress ratio (*CSR*) against the number of cycles to initiate liquefaction (N_L), or by proxy to mobilise 5% double amplitude axial strain in cyclic triaxial tests (CTX), or 3.5% shear strain in cyclic direct simple shear tests (DSS). The test data forming each curve are for a common soil, D_R and p' (or state-parameter) but varying applied amplitude of cyclic stress.

Table 1. Carbonate sand properties and origins where known

Sand (Ref.)	D_{50} (mm)	$CaCO_3$ (%)	e_{max}	e_{min}	Cu	Origins
Kurkar[1.]	0.1	-	-	-	-	-
Waikiki A[2.]	0.21	High	1.69	1.12	1.57	Coral, Hawaii
Waikiki B[2]	0.74	High	1.3	0.66	5.05	Coral, Hawaii
Dogs Bay[3.]	0.22	88-94	2.45	1.61	2.36	Shell, Ireland
Ewa Plains[4.]	0.82	98	1.3	0.66	4.1	Coral, Hawaii
Quiou[5.]	0.75	75-88	1.28	0.833	4.4	Shell, France
Kawaihae Harbor[6.]	0.6	100	1.05	0.64	-	Coral, Hawaii
Maui Dune[6.]	0.36	100	0.83	0.61	-	Coral, Hawaii
Cabo Rojo[7.]	0.38	92.8	1.71	1.34	2.1	Coral+Shell, Puerto Rico
Dubai[5.]	0.17	55	1.12	0.57	2.46	Shell, UAE
Kenya[5.]	0.13	92	1.78	1.28	1.86	Oolite, Kenya
Dabaa[8.]	0.3	High	1.04	0.75	2.4	Shell, Egypt
Nanhai[9.]	0.28	High	1.46	0.90	7.3	Coral+Shell South China Sea
Playa Santa[10.]	0.47	High	1.22	0.80	2.75	Coral+Shell, Puerto Rico
M1[11.]	0.34	>97	0.95	0.54	5.6	Shell, Persian Gulf

1. Frydman et al. (1980) cited by Pando et al. (2012)
2. Flynn (1997) cited by Pando et al. (2012)
3. Hyodo et al. (1998)
4. Morioka & Nicholson (2000)
5. Porcino et al. (2008, 2010, 2019)
6. Brandes (2011)
7. Pando et al. (2012), Moreles-Velez et al. (2015)
8. Salem et al. (2013)
9. Wang et al. (2019)
10. LaVielle (2008)
11. Giretti et al. (2018)

To compare to the liquefaction triggering curve, the CTX results have been corrected from laboratory loading conditions (isotropic confining stress, unidirectional deviatoric shear) to those in the field (anisotropically consolidated, bi-directional simple shear) by applying correction factor, C_r to the test results as (Idriss & Boulanger, 2008):

$$CRR_{\text{field}} = C_r \cdot CRR_{\text{LAB}} \tag{9}$$

where for CTX, $C_r = 0.9(1 + 2K_{0,\text{field}})/3)$, with $K_{0,\text{field}}$ being the coefficient of lateral earth pressure at-rest in the field condition. For K_0-consolidated DSS test data, only the factor of 0.9 is applied, assuming testing is conducted at similar stress conditions to the field.

The *CRR* at 15 cycles (the reference N_L used by simplified triggering method), was interpolated from the fatigue curves for each set of test results at a common D_R and p', and the K_σ factor of Idriss & Boulanger (2008) applied to normalise to 1 atm. With few exceptions, the CSL is not known for the sands for which cyclic test data are provided. Accordingly, the approach of Porcino & Marciano (2010) is followed herein, which utilises equations (3) and (5) with ξ_R forming the basis for the comparison.

Towards this end, the CPT q_c - D_R correlation (equation 2) was adopted to plot the lab-test data in CRR^* - q_{c1N} space, alongside the Boulanger & Idriss (2015) CPT-based liquefaction triggering curves for probabilities of liquefaction, P_L, of 15%, 50%, and 85% for reference. We note that at low q_{c1N} values (typ. < 80), the flatter portion of the triggering curve is characteristic of the contractive response of loose siliceous sands during shear, while at greater values of q_{c1N} the soil becomes increasingly dilative and has a correspondingly increased cyclic resistance. Due to the higher contractiveness of carbonate sands owing to their high void ratio, weak mineralogy, and angularity of particles prone to crushing, we would expect to see some difference in the position of this transition from contractive to dilative response.

Figure 4 shows that the majority of the carbonate sand cyclic test data falls between the P_L 15% and 85% triggering curves (i.e. ±1σ), with the majority of data falling in the 'contractive' region of the empirical triggering curve regardless of sample density. However, some carbonate sands indicate a transition to strongly dilatant response at a lower q_{c1N} than the empirical siliceous sand triggering curve indicates (notably Cabo Rojo and Dogs Bay calcareous sand data). If the triggering curve is converted to CRR^*-D_R space (Figure 5), using the q_{c1N}: D_R correlation for silica sands adopted by Idriss & Boulanger (2008), it is observed that the cyclic test results imply lower cyclic resistance than the triggering curve at high D_R.

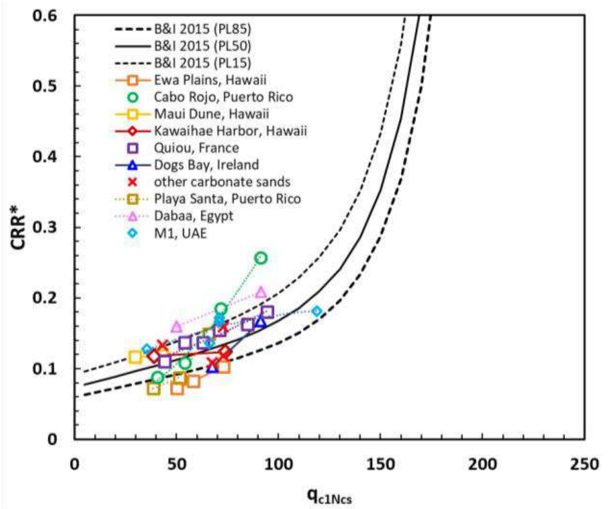

Figure 4. Collated cyclic test data plotted on the liquefaction triggering chart of Boulanger & Idriss (2015).

This appears to show a strong difference in contractiveness of the carbonate sand as compared to silica sands of the same D_R and further implies that application of an *SCF* to generate 'silica equivalent' values on the basis of D_R equivalence may not necessarily achieve equivalence in terms of cyclic resistance, and further that this assumption appears to be unconservative for dense specimens. However, it may also indicate that the behaviour of dense soils in the field, as represented by the empirical triggering curve, is not well represented by laboratory based testing, as immediately following initial liquefaction the performance of dense sands is strongly dilative on shearing, inhibiting fluidisation and surface manifestations – the characteristic required to generate observations of triggering occurrence in the field.

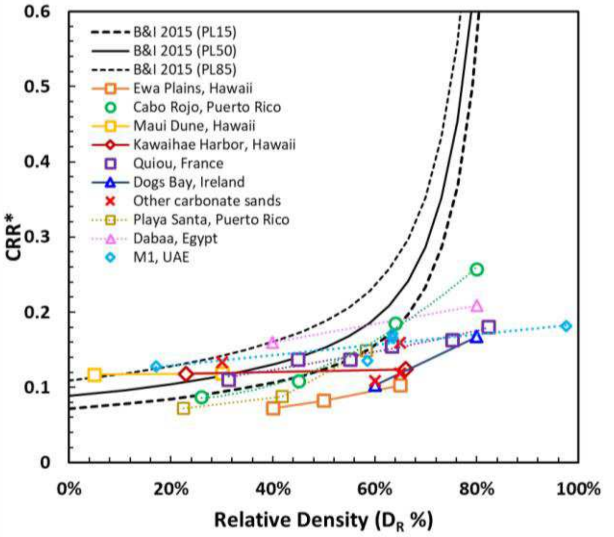

Figure 5. Collated cyclic test data with the liquefaction triggering chart of Boulanger & Idriss (2015) transposed in terms of Relative Density

Finally, a state-based approach is adopted to compare the empirical triggering curve and cyclic test data in CRR*- ξ_R space (Figure 6), following the example of Porcino & Marciano (2010). It is hypothesized that this simple conversion, using the generic CSL per equation (3), will capture the overall shift from contractive to dilative tendencies of calcareous sand versus silica sands. The cyclic test data when overlaid on the empirical triggering curve in the state-based frame of reference aligns more closely than previous references considered (q_{c1N}, D_R). This is evidenced by most of the test data plotting within ±1σ of the empirical triggering model (i.e. P_L 15% – 85%). The transition between low cyclic resistance, corresponding to low density/ contractive response, to high cyclic resistance, corresponding to high density/ dilative response, is generally captured well for those sands exhibiting a strong increase in *CRR* with reduction in ξ_R. For others, the transition is not clearly observed either due to lack of data at high densities or some other cause such as inaccuracy in CSL estimation, or weaker grains that are more susceptible to crushing during cyclic loading of denser specimens, or other differences between field and laboratory response as noted earlier.

Overall, however, the reasonably close comparison of the carbonate sand test data and the semi-empirical triggering curve after the state-based corrections are applied indicates that most differences between the behaviour of silica and carbonate sands have been appropriately considered when evaluated in accordance with a state-based framework.

3.2 *State based triggering curve*

As the state-based framework appears to better align with the calcareous sand dataset, a correlation between q_{t1N} and ξ_R was considered. This bypasses the use of D_R as a go-between, even though it introduces some additional uncertainty. The following expression is derived from equations (2), (3) and (5):

$$\xi_R \approx 1.407 - 0.558 \cdot {q_{t1}}^{0.264} \qquad (10)$$

A correlation between SPT N and q_c is required to utilise equation (10) with SPT data, which may be achieved through equating D_R in equations (2) and (7):

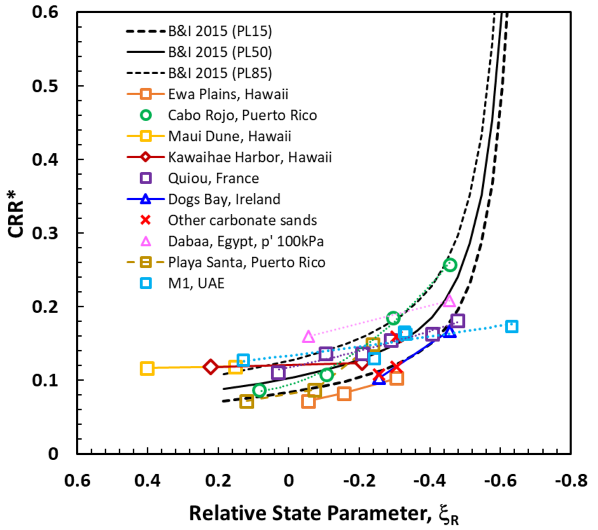

Figure 6. Collated cyclic test data with the liquefaction triggering chart of Boulanger & Idriss (2015) transposed in terms of Relative State Parameter.

$$q_{t1} \approx 9.12\left(0.1474\sqrt{(N_1)_{60}} + 1.222\right)^{3.788} \qquad (11)$$

The deterministic simplified liquefaction triggering curve (P_L 15%) from Boulanger & Idriss (2015) may be expressed in terms of relative state parameter as follows:

$$CRR^* = EXP(-44.417\xi_R^5 - 37.624\xi_R^4 - 5.602\xi_R^3 + 3.820\xi_R^2 - 0.988\xi_R - 2.673) \qquad (12)$$

This approach is used to evaluate liquefaction case histories from the 1993 Guam and 2010 Haiti earthquakes. As shown in Figure 7, all of the cases are correctly predicted using the procedure.

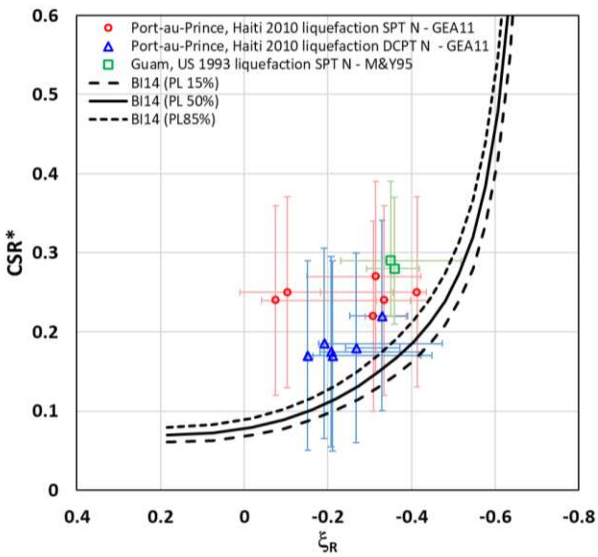

Figure 7. Liquefaction case histories from 1993 Guam & 2010 Haiti earthquakes plotted on the Boulanger & Idriss (2015) triggering curve transposed in terms of Relative State Parameter.

3.3 *Shear wave velocity-based corrections*

An appraisal of published laboratory cyclic testing for which V_S measurements were made using bender-elements suggests V_S data on reconstituted carbonate sands is ~1.3× higher than silica sands having the same cyclic resistance (Porcino & Tomasello, 2019). This may be due to the higher mineral friction angle, ϕ_μ, where $\phi_{\mu,calc}$ ~1.35 × $\phi_{\mu,quartz}$ (Jamiolkowski et al. 2001). This factor matches the observations from field tests wherein V_S and CPT were performed, followed by blast-induced liquefaction tests in Hawaii (Rollins et al. 2004). A simple linear reduction factor to field V_S data (i.e. 1/1.3) before applying to the V_S-based simplified triggering assessment is recommended. These results do not consider the influence of aging and cementation which may further affect this ratio and would be expected to confer higher liquefaction resistance to natural soil deposits.

4 CONCLUSIONS

Published calibration chamber data for carbonate sands have been reviewed, and state-concepts adopted to infer suitable corrections to SPT and CPT test results in order to apply the simplified liquefaction triggering method. A state-based framework is further investigated as a suitable means to assess liquefaction triggering through comparison with published cyclic test results on an array of carbonate sands. However, questions remain about the response of these soils at very high densities, and further testing that captures field-like responses (e.g. shake table or centrifuge testing) may yield new insights. A proposed relationship is presented to estimate the relative state parameter, ξ_R, from CPT and SPT data, and to transpose the simplified triggering curve in terms of ξ_R. Application of this method to the 1993 Guam and 2010 Haiti case history data indicates it provides reasonable interpretation compared to field observations.

5 REFERENCES

Al-Homoud, A.S., and Wehr, W., 2006. Experience of vibrocompaction in calcareous sands of UAE. *Geotech. & Geol. Eng.*, 24: 757-774.

Almeida, M.S.S., Jamiolkowski, M., and Peterson, R.W. Preliminary result of CPT tests in Calcareous Quiou Sand. *Proc. Int. Symp. Calibration Chamber Testing*, Potsdam, New York, 1991. Elsevier, pp. 41-53.

Been K. & Jefferies M.G. 1985. A state parameter for sands. *Géotechnique,* 35(2): 99-112.

Bellotti, R., and Jamiolkowski, M., 1991. Evaluation of CPT and DMT in crushable and silty sands, 3rd interim report ENEL, C.R.I.S., Milano (cited by Al-Hamoud & Wehr, 2006).

Bolton M.D. 1986. The strength and dilatancy of sands. *Géotechnique* 36(1), 65-78.

Boulanger R.W. 2003 Relating Kα to Relative State Parameter Index. *Journal of Geotech. & Geoenviron. Eng.* 129 (8), 770-773.

Boulanger, R.W. and Idriss I.M., 2015. *CPT-based Liquefaction Triggering Procedure*. J. Geotech & Geoenv. Eng. 142(2)

Brandes, H.G., 2011. Simple shear behaviour of calcareous and quartz sands. *Geotech. & Geol. Eng.*, 29:113-126.

Coop M.R., 1990. The mechanics of uncemented carbonate sands. Géotechnique 40(4), 607-626.

Coop, M.R., and Atkinson, J.H. 1993. The mechanics of cemented carbonate sands. *Géotechnique* 43(1): 53-67.

Fioravante, V., Cappferri, R., Hameury, O., Jamiolkowski, M, 1994. Deformational characteristics of uncemented Quiou sand. Proc. Int. Symp. Pre-failure Deform. Charact. of Geom., Sapporo: 55 – 61.

Fioravante, V., Giretti, D., and Jamiolkowski, M. 2013. Small strain stiffness of carbonate Kenya Sand. *Engineering Geology* 161, 65-80.

Fioravante, V., Jamiolkowski, M., Ghionna, V.N., Pedroni S., 1998. Stiffness of carbonate Quiou sand from CPT. In: Robertson, Mayne (Eds), *Proc. 1st Int. Conf. Site Characterisation*, pp. 1039 – 1049.

Giretti, D., Been, K., Fioravante, V. & Dickenson, S. (2018b). CPT calibration and analysis for a carbonate sand. *Géotechnique* 68 (6), 345–357.

Giretti, D., Fioravante, V., Been, K. & Dickenson, S. (2018a). Mechanical properties of a carbonate sand from a dredged hydraulic fill. *Géotechnique* 68 (5), 410–420.

Golightly C.R. and Hyde A.F.L. 1988. Some fundamental properties of carbonate sands. *Eng. for Carb. Sediments*. Balkema, Rotterdam.

Green, R.A., Olson S.M., Cox, B.R. et al. 2011. Geotechnical Aspects of Failures at Port-au-Price Seaport during the 12 January 2010 Haiti Earthquake. *Earthquake Spectra*, 27(S1): S43-S65.

Hyodo, M., Hyde, A.F.L., and Aramaki, N., 1998. Liquefaction of Crushable Soils. *Géotechnique*, 48(4): 527-543.

Idriss, I.M., and Boulanger R.W., 2008. *Soil Liquefaction During Earthquakes*. Oakland, California: EERI.

Jamiolkowski, M., Lo Presti, D.C.F. and Manassero, M. 2001. Evaluation of Relative Density and Shear Strength of Sands from CPT and DMT. *Soil Behaviour and Soft Ground Construction*. Geotechnical Special Publication No. 119, ASCE: 201-238.

Jefferies M., and Been K. 2006. *Soil liquefaction. A critical state approach*. Taylor & Francis.

LaVielle, T.H. 2008. Liquefaction susceptibility of uncemented calcareous sands from Puerto Rico by cyclic triaxial testing. MS Thesis. Virginia Polytechnic Institute and State University.

Lees, A., King, D.A., and Mimms, S. 2013. Palm Jumeirah, Dubai: cone penetrometer testing data from the carbonate sand fill. *Geotech. Eng.* 166 (GE3), 253-267.

Mayne, P.W. 2014. Interpretation of geotechnical parameters from seismic piezocone tests. *Proc. 3rd Int. Symp. CPT,* Las Vegas,47-73.

Medley, E.W., 2006. *Geological Engineering Reconnaissance of Damage Resulting from the October 15, 2006 Earthquakes, Island of Hawaii, Hawaii, USA*. Oakland (CA): GEER Association.

Mejia, L.H., and Yeung, R., 1995. Liquefaction of Coralline Soils During the 1993 Guam Earthquake: In: *Earthquake-Induced Movements and Seismic Remediation of Existing Foundations and Abutments*. Geotechnical Special Publication No. 55, ASCE: 33- 48.

Mengé, P., Vinck, K., Van den Broeck, M., et al. 2016. Evaluation of relative density and liquefaction potential with CPT in reclaimed calcareous sand. In: *Geotech. & Geophys. Site Charact. 5*. Lehane, Acosta-Martinez & Kelly (Eds). AGS, Sydney, Australia.

Morales-Velez, A.C., Baxter, C.D.P., and Pando M.A., 2015. Evaluation of the cyclic resistance of an uncemented calcareous sand deposit from Puerto Rico using Shear Wave Velocity. *Proc. 6th Int Conf Earthq. Geotech. Eng.*, Christchurch, N.Z.

Morioka B.T., and Nicholson, P.G., 2000. Evaluation of the Liquefaction Potential of Calcareous Sand. *Proc. 10th Int. Offshore and Polar Engineering Conference*, Seattle, USA. Vol. II: 494- 500.

Nicholson P.G., 2006. Liquefaction evaluation discrepancies in tropical lagoonal soils. *Geotech. & Geol. Eng.* 24: 1259 – 1269.

Pando, M.A., Sandoval, E.A., and Catano, J., 2012. Liquefaction Susceptibility and Dynamic Properties of Calcareous Sands from Cabo Rojo, Puerto Rico, *Proc. 15th World Conf. Earthq. Eng.*, Lisbon, Portugal.

Porcino, D., and Marciano, V. 2010. Evaluating Liquefaction Resistance of a Calcareous Sand Using the Cone Penetration Test. *Proc. 5th Int. Conf. Recent Adv. Geotech. Earthq. Eng. and Soil Dyn*. San Diego.

Porcino, D., and Tomasello, G., 2019. Shear wave velocity-based evaluation of liquefaction resistance for calcareous sands of different origin. *Soil Dynamics and Earthquake Engineering*. 122: 235-247.

Porcino, D., Caridi, G., and Ghionna, V.N., 2008. Undrained monotonic and cyclic simple shear behaviour of carbonate sand. *Géotechnique*, 58(8): 635-644.

Poulos, H.G., 1988. The Mechanics of Calcareous Sediments. *Australian Geomechanics*, Special Issue, 5th ANZ Geotechnics Conference, Sydney. pp. 8 – 41.

Randolph M.F., Jamiolkowski M.B., and Zdravkovic L. 2004. Load carrying capacity of foundations. Proc. Advances in Geotech. Eng.: Skempton Memorial Conf., London UK. Vol. 1: 207-240.

Rathje, E., Bachhuber, J., Cox, B., et al. 2010. *Geotechnical Engineering Reconnaissance of the 2010 Haiti Earthquake*. V1. February 22, 2010. GEER Association.

Rollins, K.M., Lane, J.D., Nicholson P.G., and Rollins, R.E., 2004. Liquefaction Hazard Assessment Using Controlled – Blasting Techniques. *Proc. 11th Int. Conf. Soil Dyn. Earthq. Eng*. 2: 630-637.

Salem M., Elmamlouk H., and Agaiby S. 2013 Static and cyclic behaviour of North Coast calcareous sand in Egypt. *Soil Dy. & Earthq. Eng.* 55: 83 – 91.

Semple R.M. 1988. The mechanical properties of carbonate soils. *Proc. Int. Conf. on Calc. Sediments*, Perth, Australia, Vol. 2: 807-836.

Van Impe, P.O., Van Impe, W.F., Manzotti, A., et al. 2015. Compaction control and related stress-strain behaviour of off-shore land reclamations with calcareous sands. *Soils Found.*, 55(6): 1474-1486.

Vesic, A.S., 1965. Ultimate loads and settlements of deep foundations in sand. *Proc. Symp. Bearing Cap. & Settlement Found. in Sand*, SMS 5, Duke Univ., Durham, 53-68 (cited by Al-Homoud & Wehr 2006).

Wang Y., Qiu Y., Ma L. and Li Z. 2019. Experimental study on the cyclic response of Nanhai Sea calcareous sand in China. *Arabian J. Geosciences*. 12:677.

Wehr, W.J. 2005. Influence of carbonate content of sand on vibro compaction. *Proc. 6th Int. Conf. ground improve. techn.*, Portugal.